Chapter 3
Investigating Three-Axis Shock and Vibration with a "Supplemental Shaker" Frame

R. Krieghbaum and S. M. Danforth

Abstract Traditional single-axis environmental testing methods have been shown to over-test components by means of cross-axis excitation, leading to potential damage to test objects that would not be experienced in the field. Multi-input, multi-output testing seeks to address cross-axis excitation by controlling all principal axes during the test, but these methods have had difficulty reaching high-amplitude flight environments. This paper seeks to explore a new method of multi-axis excitation, using a large shaker for axial excitation with additional "supplemental" shakers in the remaining principal axes. A test frame was designed to enable attachment of two supplemental shakers. The test frame was evaluated by subjecting a representative test assembly to transport vibration, flight vibration, and flight shock environments, and these results are compared to a similar test completed using single-axis methodology.

Keywords Environmental shock and vibration testing · Multi-axis shock and vibration testing · Flight environments

Abbreviations

DOF – Degree of freedom
GOBLET – Generic OBject for Laboratory Environmental Testing
PSD – Power spectral density
GRMS – Root-mean-square acceleration, in units of g
SRS – Shock response spectrum
LANL – Los Alamos National Laboratory
MIMO – Multi-input, multi-output
SISO – Single-input, single-output

Introduction

The Shock and Vibration Team at Los Alamos National Laboratory (LANL) seeks to recreate environments of test objects as accurately as possible in a laboratory setting as an alternative to the costly process of performing field tests. Current qualification test methods use single-input, single-output (SISO) testing, where test objects are excited using a single shaker and rotated for sequential excitation in all three principal axes. This test method has been preferred because of the requirement of high excitation levels, such as those experienced during flight stages, that only large, single-axis shakers can provide. However, constraining test articles to single-axis testing may fail to accurately depict the multi-axis forces present during field environments, such as aerodynamic loading that occurs during flight environments and rocket propulsion. Additionally, segmenting test environments into sequential SISO tests has shown to result in cross-axis excitation, yielding elevated excitation levels from the environment specification [1]. Excitation greater than the environmental specification may produce excess damage to production components that would not be experienced during the lifetime of the component.

R. Krieghbaum · S. M. Danforth
Bikini Atoll Rd, Los Alamos, NM 87544
e-mail: rkrieghbaum@lanl.gov; sdanforth@lanl.gov

© The Author(s), under exclusive license to River Publishers 2026

Kristin B. Zimmerman, PhD (eds.), *Dynamic Environments and Durability Testing, 2026, Vol. 7*, Conference Proceedings of the Society for Experimental Mechanics Series, https://doi.org/10.13052/rp-9788743814184

Multi-input, multi-output (MIMO) testing has been shown to provide more field-relevant boundary conditions and address cross-axis excitation concerns by controlling to multiple degrees of freedom (DoFs) using multiple excitation sources during a single test [1]. One method of MIMO excitation uses multiple small, distributed shakers to recreate distributed-loading environments [2]. While this method of MIMO testing addresses current environment replication concerns, the smaller shakers used in these tests are often incapable of supplying the necessary excitation for high-amplitude flight environments.

In previous work, LANL test engineers aimed to address the low excitation levels of distributed shaker testing by using a high-force-output, single-axis shaker for axial excitation and a smaller modal shaker for lateral excitation [3]. We labeled this method as "supplemental shaker" testing because the smaller lateral shaker(s) could supplement the high force provided in the axial direction. The previous supplemental shaker studies showed promising multi-axis control performance for both flight and transportation environments. However, the excitation was limited to two axes because the test area did not have room to suspend a second supplemental shaker.

In this paper, we build upon previous research by introducing a custom test frame that can suspend multiple small shakers with a compact footprint, enabling supplemental shaker testing for flight environments in the three principal axes of a test body. Our goal is to compare the acceleration response of a representative test assembly between three-axis supplemental shaker testing and traditional single-axis testing, with a focus on analyzing viability of the new test method. In Section 2.0, we introduce the test assembly and three test environments that are of interest to LANL's weapons programs. Section 3.0 describes the test frame used during testing, including its features and design considerations. Sections 4.0 and 5.0 describe the equipment, procedure, and notable events experienced during single-axis and multi-axis testing, respectively. Test results are reported in Section 6.0, with discussion presented in Section 7.0 and overall conclusions presented in Section 8.0.

Test Article and Proposed Test Environments

In this study, we conducted testing on an article called the GOBLET (Generic OBject for Laboratory Environmental Testing). The GOBLET was designed to investigate the coupling dynamics of a rigid and compliant component, shown in Figure 1. Part A is thin and bell-shaped, making it compliant when coupled with Part B, a rigid cylinder. A fixture plate was used to attach the GOBLET to the shaker armature or slip table for environmental shock and vibration testing.

Part A of the GOBLET was connected to Part B using three bolted "legs." This study uses the leg oriented 270° clockwise from the +Y direction, referred to as the "270 Leg," as a location for control. In addition to instrumenting the 270 Leg, we

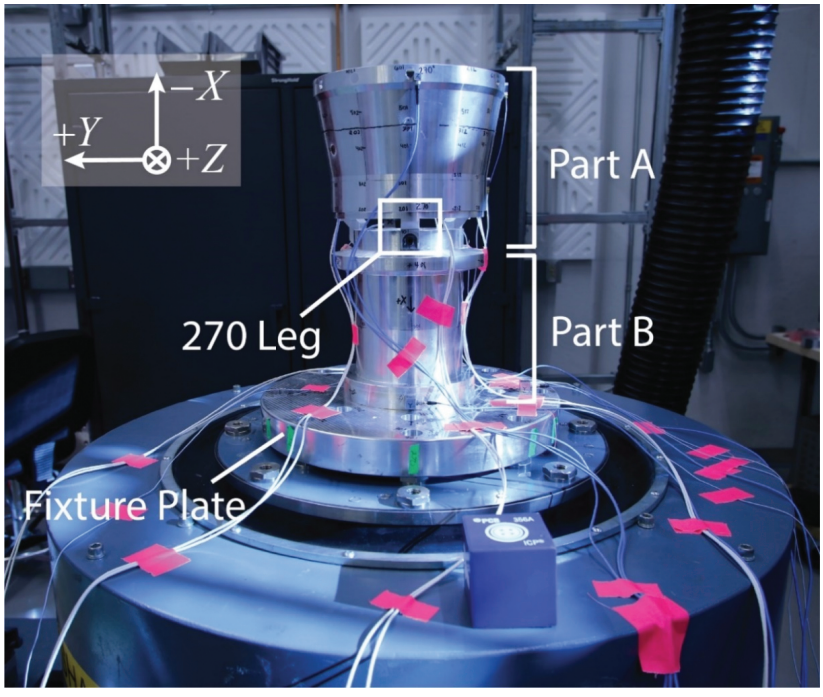

Fig. 1 Overview of the GOBLET test assembly with system axes and notable locations specified

placed accelerometers (PCB and Endevco, 22 channels) and strain gauges (Vishay Measurements Group, 8 channels) at other locations throughout Part A, Part B, and the fixture plate. These extra sensors will aid in evaluating differences in global test article response between testing methods, although the strain data are not evaluated in this study.

We selected three environments for our initial evaluation of the supplemental shaker test frame: a Transport Random vibration environment, Flight Random vibration environment, and a Flight Shock environment. The Transport Random environment contains lower-level transportation vibrations with a higher makeup of low-frequency content, yielding larger displacements that pose a challenge to the supplemental axes. Additionally, LANL team members successfully tested the Transport Random environment at a truncated frequency range in previous two-axis supplemental shaker work, and additional testing of this specification will enable comparison to previous methods [3]. The Flight Random environment contains higher excitation levels with broader frequency content, challenging the capacity of the supplemental shakers to provide sufficient drive voltage in their respective axes. Finally, the Flight Shock environment was chosen because LANL test engineers have not yet attempted multi-axis shock and sought to evaluate its viability in the supplemental shaker test method. When compared to vibration environments, shock environments often involve high displacement, pose unique control challenges, and exacerbate nonlinear system behavior. The Flight Shock environment represents a low-level shock, yielding a reasonable starting point for exploring use of supplemental shakers for MIMO shock testing.

Both random vibration environments, Transport Random and Flight Random, are implemented in the laboratory by controlling to power spectral densities (PSDs) in the frequency domain. The average amplitude of vibration signals synthesized using these PSDs can be estimated by integrating each PSD over its frequency range and taking the square root of the result, yielding the GRMS (root-mean-square acceleration, in g) value for the profile. Figure 2 shows plots of these PSDs along each DoF at the 270 Leg, and Table 1 provides the GRMS of each environment. The SISO testing described in Section 4.0 controls each DoF sequentially, while the supplemental MIMO testing described in Section 5.0 controls the DoFs simultaneously. Note that the PSDs specified in this section are auto spectral densities, but in MIMO testing, cross power spectral densities additionally play a role in environment specification. Our approach to addressing the cross powers is described in Section 5.0.

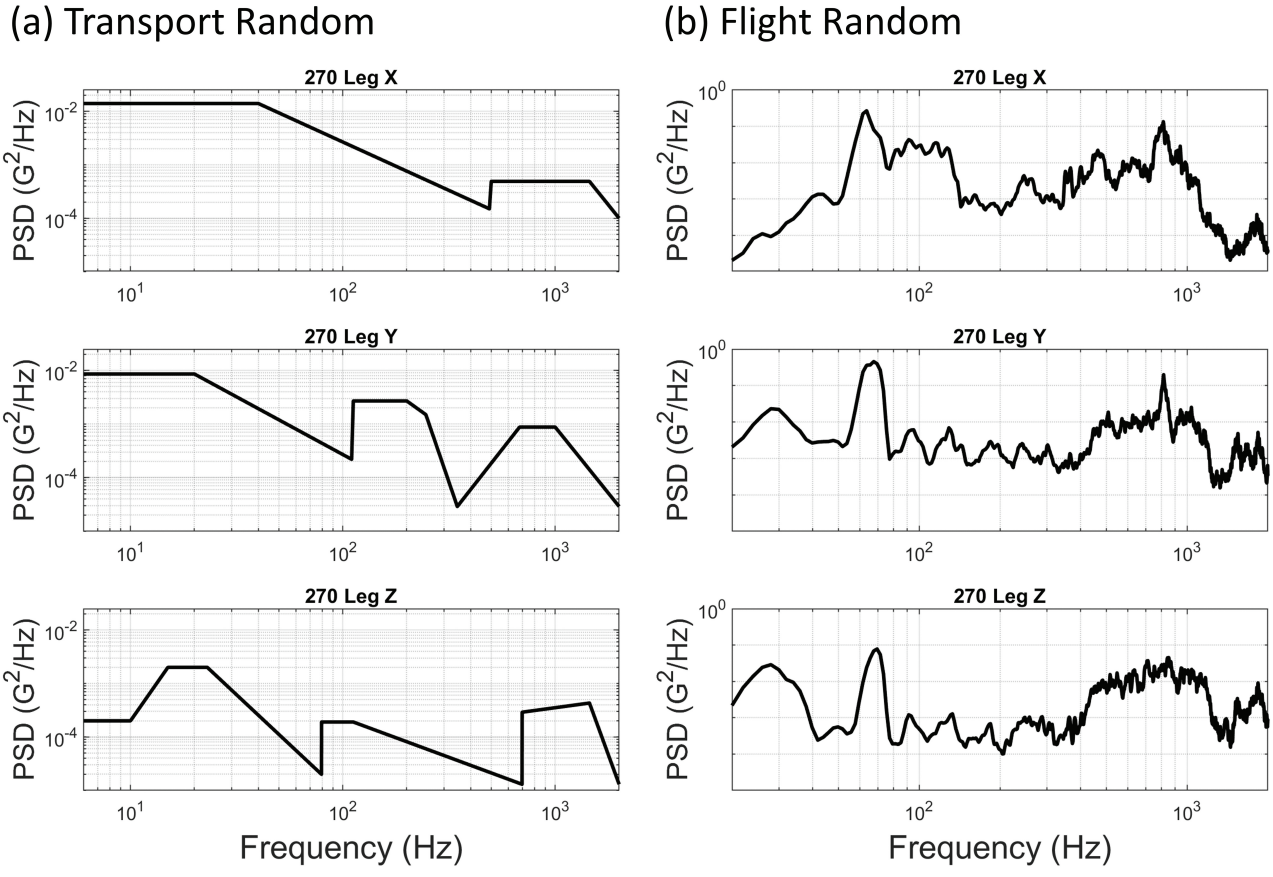

Fig. 2 Random vibration environments used during testing, specified at the principal axes of the 270 Leg

Table 1 GRMS Values for Random Vibration Environments

Environment Name	Frequency Range (Hz)	Axis	GRMS
Transport Random	6–2000	X	1.29
		Y	1.11
		Z	0.64
Flight Random	20–2000	X	3.89
		Y	4.16
		Z	3.63

The Flight Shock environment is specified as a shock response spectrum (SRS) maxi-max absolute acceleration (MMAA), shown in Figure 3(a) for X, Y, and Z at the 270 Leg from 20 Hz–2000 Hz [4]. We worked with the V-14 Data Analysis Team to synthesize a time waveform that achieves this SRS profile. Figure 3(b) shows the synthesized time waveforms for the Flight Shock environment for X, Y, and Z at the 270 Leg.

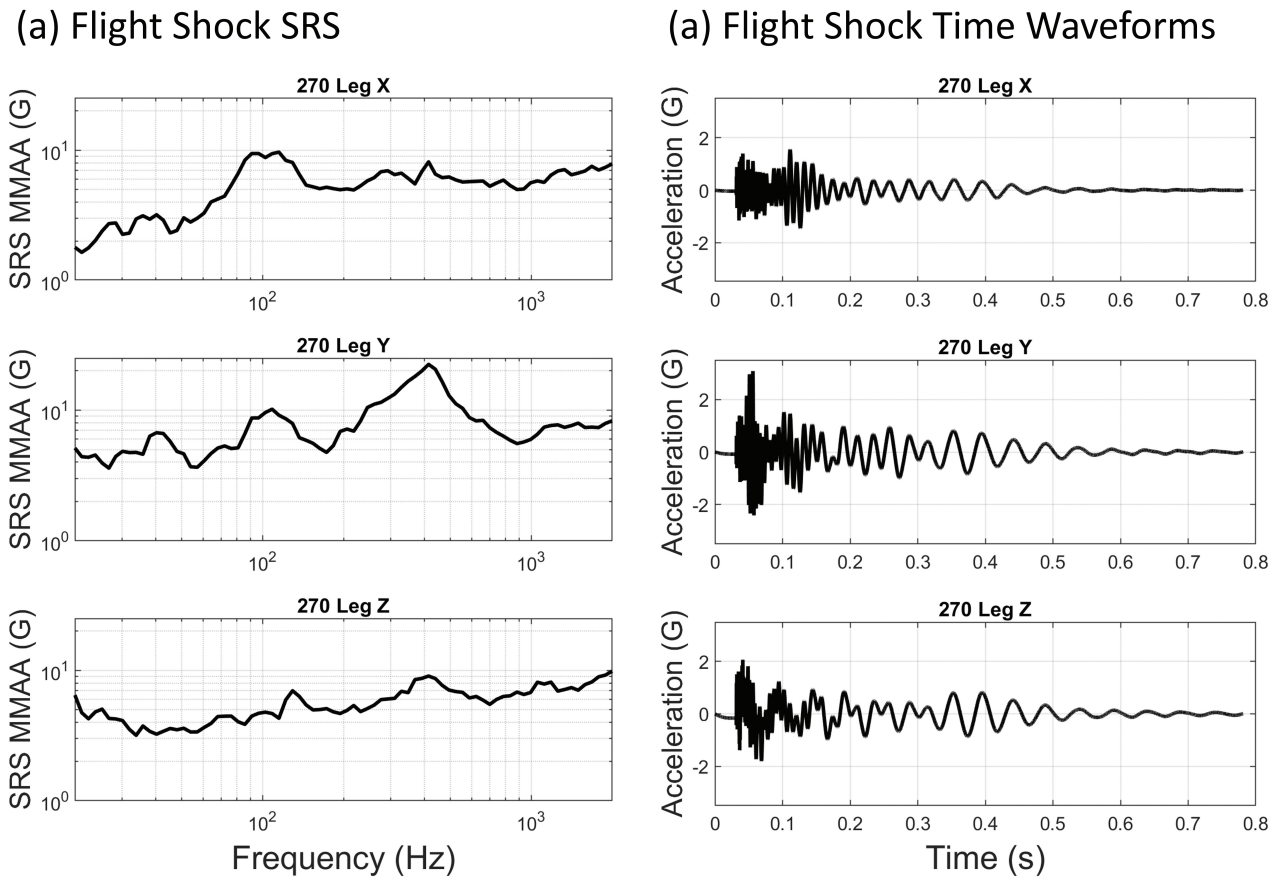

Fig. 3 Shock environment (a) SRS and (b) Time Waveforms used during testing, specified at the principal axes of the 270 Leg

In addition to evaluating control performance, we are interested in comparing system response at non-control locations between single-axis and supplemental test methods. We selected the X, Y, and Z channels of Point 2504 as response DoFs, since Point 2504 is located close to the rim of Part A of the GOBLET. With Part A's bell-like characteristics, we expected interesting motion amplification between our control DoFs at Point 2101 and the response DoFs at Point 2504. Figure 4 highlights Point 2504's location relative to Control Point 2101.

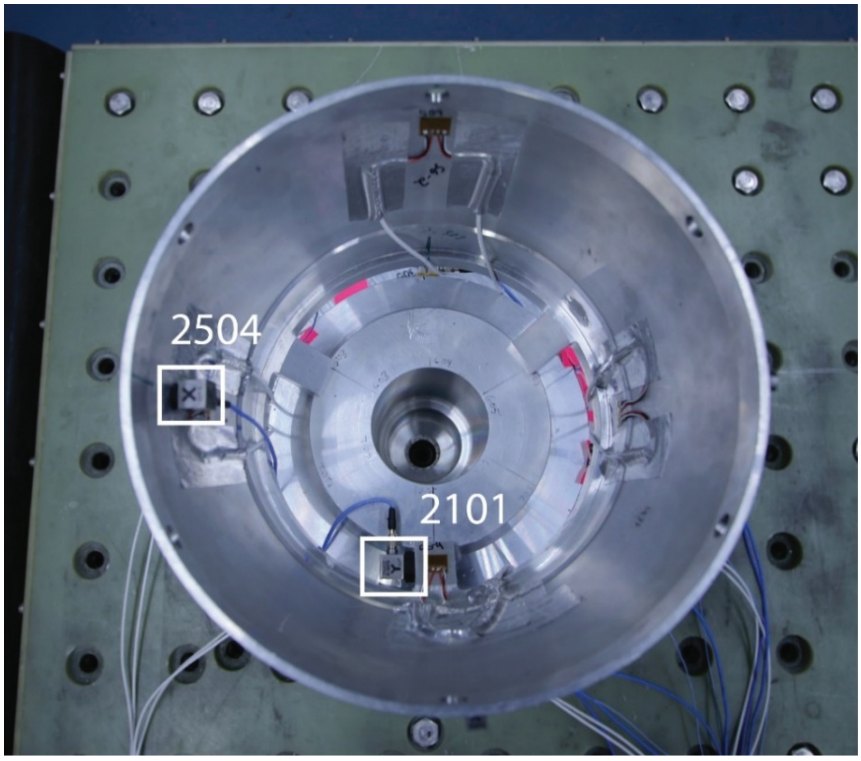

Fig. 4 Locations of Point 2504, near the rim of Part A, and Control Point 2101, located on the 270 Leg

Test Frame Design

As with previous supplemental shaker studies, we identified the Unholtz-Dickie H560 shaker as the large shaker for providing axial excitation. This shaker does not have an associated slip table, which provided more room for a supplemental test frame. Previous supplemental shaker testing used a Lateral Excitation Stand from The Modal Shop to suspend one Modal Shop 2100E11 100-lbf shaker for supplemental excitation [3]. This excitation stand was difficult to reconfigure around the H560 shaker, and because of the size of the stand, only one supplemental shaker was capable of being suspended. To enable the use of multiple shakers from both fixed and suspended attachment as well as increased movement of the small shakers around the test object, we designed a test stand for future multi-axis testing.

The general layout of the test frame is shown below in Figure 5(a), with an approximate size of 6x6x6 ft and weight of 500 lb. The frame consists of Bosch-Rexroth 90x90L aluminum extrusion forming an external structure with "tree-and-branch" internal structures enabling shaker alignment. The "trees" refer to the vertical beams spanning the height of the frame, which can be moved laterally, and the "branches" refer to the cantilevered beams that hold the shakers. The branch height can be adjusted, and multiple branches can be added to each tree if more than one shaker is desired in each axis. We chose the general frame design after discussion with Sandia National Laboratories, who implemented a similar frame design and noted the benefits of high maneuverability for smaller shakers. We selected the 90x90L profile on the recommendation of the manufacturer of the frame, Pacific Integrated Handling, who was provided with the intended shaker size, weight, and applications the frame would experience. In a previous project, we designed a frame with 2-in. aluminum extrusion, but because of scheduling issues, the frame was not used in testing. While assembling the previous frame, V-14 engineers noted high displacements from manual excitation, providing further motivation for the use of 90x90L in the new test frame.

The test frame enables three-dimensional (3D) positioning of the supplemental shakers by means of movement of the vertical support beam (tree), movement of the horizontal arm (branch), and movement of the adapter plate along the arm. We purchased additional lengths of extrusion to enable further adjustment of the shaker's proximity to the test object and avoid interference with larger test objects. Machined $\frac{1}{4}$-in. aluminum adapter plates rigidly mount the trunnions of the shakers to the frame and can be placed on any surface of the horizontal arm. Additionally, these adapters may be used to suspend the shakers below the horizontal arm if non-rigid attachment proves beneficial for shaker isolation. Figure 5(b) shows an implementation of the supplemental shakers on a mock single-axis shaker, with indicator arrows highlighting adjustment capabilities.

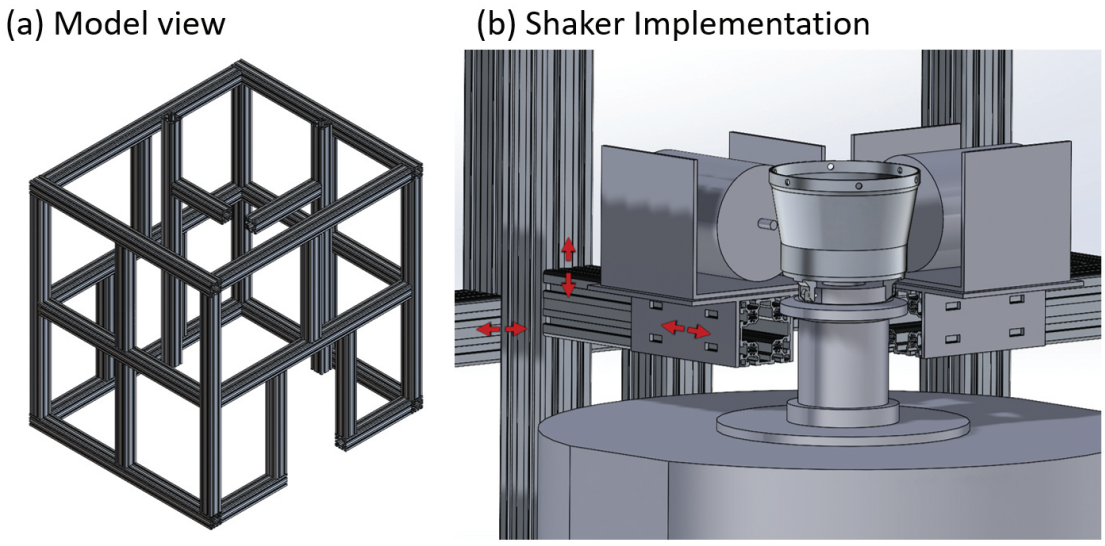

Fig. 5 Supplemental frame design, showing (a) an isometric view of the test frame and (b) mounted shakers with arrows indicating adjustment capabilities

We also purchased rubber padding and additional stiffening gussets to explore optimization of the dynamic characteristics of the test frame. Previous research found that while the dynamics of the test article are the greatest contributing factor in MIMO control efficacy, modification of the dynamic characteristics of the test frame did yield notable change in test performance [5]. These changes are not currently well-understood and may be amplified or reduced by factors such as test frame size, frame or supplemental shaker weight, test environment levels, and any shaker-frame coupling present in the shaker attachment method for a given test setup. Use of these additional components and attachment methods could increase the overall stiffness and damping of the test frame, which may enable alteration of high-amplitude resonances experienced by the test frame during testing.

Single-input, Single-output Testing

We conducted SISO shock and vibration tests on the GOBLET for a baseline comparison to the planned multi-axis supplemental shaker tests. All single-axis tests were conducted using the Unholtz-Dickie S452 shaker. The S452 (SISO tests) and H560 (MIMO tests) differ in characteristics, but we were comfortable using the S452 as a comparison because our goal was to compare a traditional test method to a new one rather than compare SISO versus MIMO with identical shakers.

We first ran the X-axis test with the S452 in its vertical configuration, then we ran the Y- and Z-axis tests with the shaker rotated horizontally and attached to the slip table. We torqued all socket head cap screws between the fixture plate and shaker armature or slip table to the same specification in each axis to ensure similar boundary conditions. Figure 6 shows the SISO test setups for each axis.

In all SISO tests, we used Simcenter Testlab software for control and Simcenter SCADAS hardware for data acquisition. For safety and data quality purposes, Simcenter Testlab allows the user to specify alarm and abort profiles above and below the reference PSD. In LANL qualification tests, we specify alarm profiles at ± 3 dB and abort profiles at ± 6 dB and direct Simcenter Testlab to stop the test if the computed test PSD exits the alarm or abort limits for 5% or 3% of frequency lines, respectively.

The S452 was able to achieve the Transport Random vibration environment for the full frequency range (6 Hz–2000 Hz) in all three axes. The Flight Random vibration environment was successful for the full frequency range (20 Hz–2000 Hz) in the X- and Y-axes, but we had to truncate the Z-axis frequency range to 20 Hz–1000 Hz. Above 1000 Hz, system resonances caused the test PSD to exit the abort limits for greater than 3% of frequency lines. After truncating the environment, the test satisfied our qualification control criteria. We achieved the Flight Shock environment but had the most difficulty with the X-axis waveform, which has the lowest acceleration magnitude.

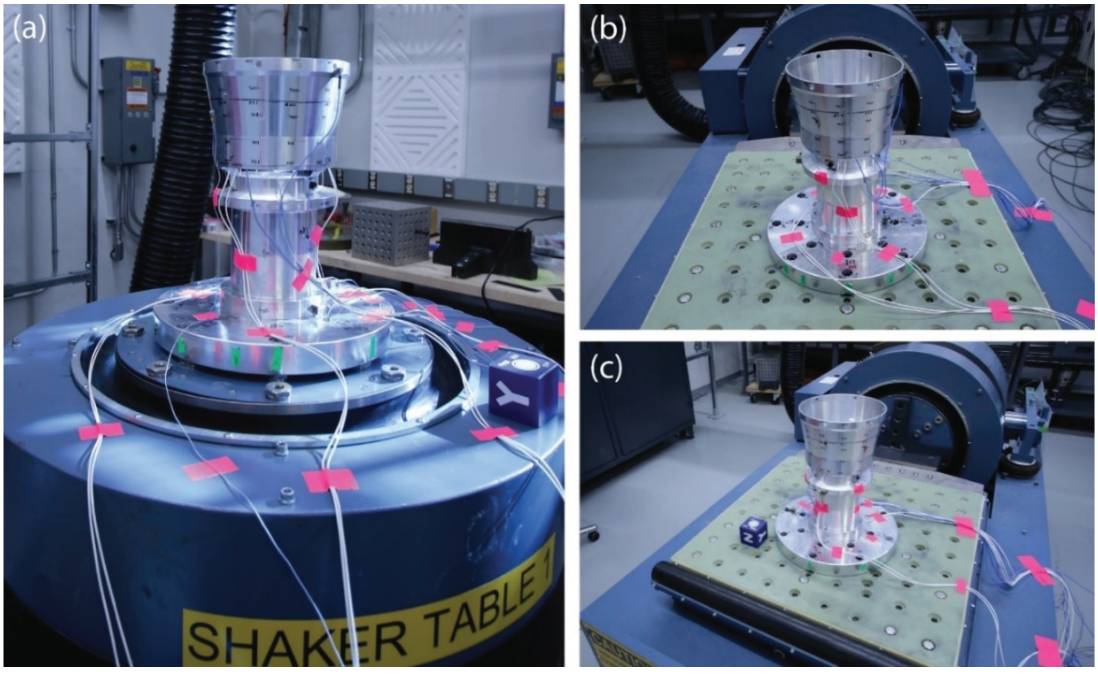

Fig. 6 Single-axis testing setups on the S452 shaker in the (a) X-axis test, (b) Y-axis test, and (c) Z-axis test

Multi-input, Multi-output Testing

After constructing the supplemental shaker frame, we conducted multi-axis testing over a 2-week period. The Unholtz-Dickie H560 shaker provided X-axis excitation, and two 110-lbf shakers (2110E from The Modal Shop) provided excitation in the Y- and Z-axes. We used Simcenter Testlab software and Simcenter SCADAS data acquisition hardware for all multi-axis tests. Each supplemental shaker imparted force through a compliant metal rod called a stinger that was threaded into a load cell, which was in turn threaded into a 3D-printed drive block. The drive block attached to the GOBLET using dental cement (DuraKore, Reliance Dental MFG and X60 Cold Curing Glue, HBK).

Before conducting a shock or vibration test, the Simcenter Testlab software completes a System Identification step. In this step, the controller outputs uncorrelated drive voltage signals to each shaker's amplifier at a flat, low-level PSD that spans the intended testing frequency spectrum. It then measures the response at the control DoFs (2101 X, Y, and Z) and computes system frequency response functions (FRFs). Using these FRFs, the software predicts whether the environment can be achieved by the shakers without exceeding the allowable drive voltage limits (10 V). If the environment requires too much drive voltage, we truncate the frequency range until the test is achievable.

Unlike the SISO tests, we relaxed the alarm/abort limit percentages to allow for test completion. Because the addition of multiple excitation sources and control DoFs creates a more challenging control problem, it is likely that the 5%-alarm and 3%-abort limits will need to be adjusted for MIMO qualification tests, but there has been no investigation into what percentage of excursion is allowable.

In Section 2.0, we presented the auto PSDs for the multi-axis test. In MIMO tests, cross power spectral densities (CPSDs), which describe the co-variance between two signals, are also present. The Simcenter Testlab software has two multi-input control modes: "Matrix" and "PSD." In Matrix mode, the user specifies CPSDs as a matrix at each frequency line. Because CPSDs are not currently included in the specification development process, the common practice within the Department of Energy Complex is to compute the CPSDs during the System Identification step, then populate the specification with the in-situ CPSD values. In PSD mode, the user specifies only the auto PSDs for control and allows in-situ CPSD population.

For our first test series with the supplemental shaker frame, we tried implementing Matrix mode control with the CPSDs from the System Identification step. However, the predicted required drive voltage levels were too high. We switched to PSD mode, which reduced the required drive voltage for the supplemental shakers. All results in Section 6.0 report auto PSD results from PSD mode control. Future work will make additional attempts to control using Matrix mode.

We began testing with the two supplemental shakers rigidly attached to the test frame branches (Figure 7(a)) and the drive blocks attached to Part B, the rigid cylinder, of the GOBLET. First, we ran the Transport Random environment. Although the Transport Random environment specification was defined from 6 Hz–2000 Hz in Section 2.0, we could not reach the low-

frequency, high-displacement values with our MIMO setup. This limitation was expected as displacements in a multi-input test cause shaker misalignment. We therefore truncated the environment to 20 Hz–2000 Hz. Despite truncating the lower frequencies, the rigid shaker attachment caused excessive, visible frame displacement during testing. We re-configured the test setup to have bungee attachment (Figure 7(b)) and were able to complete the transportation environment from 20 Hz–2000 Hz.

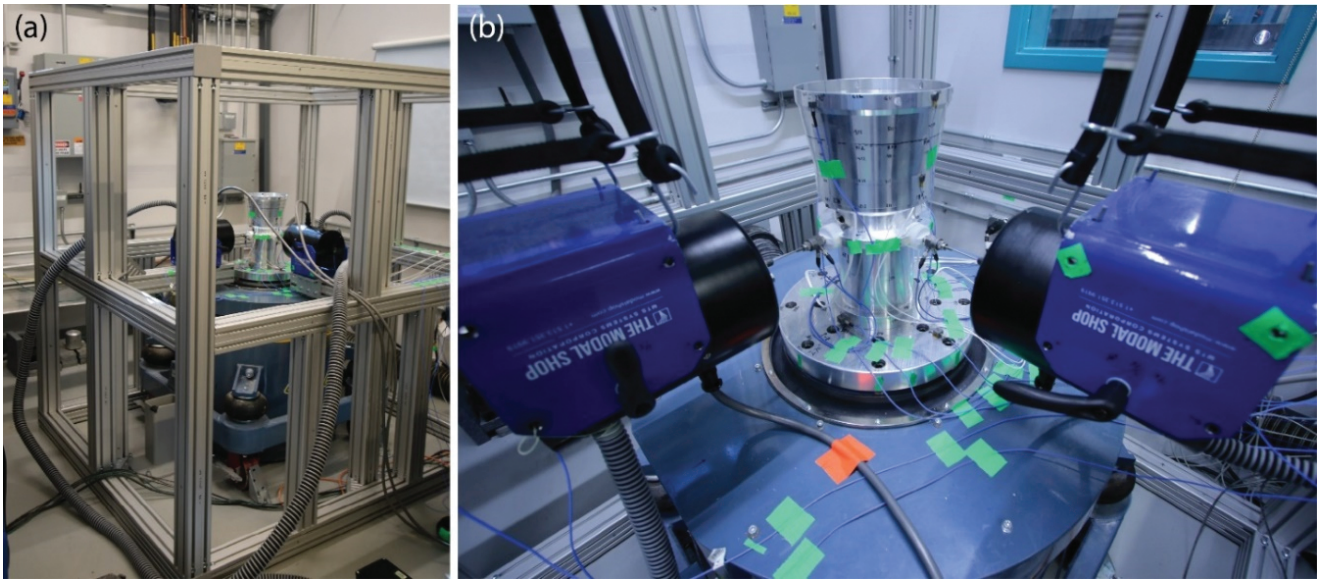

Fig. 7 In-situ test setup showing (a) the assembled frame, and (b) suspended supplemental shakers

Early in testing, we noticed that the print quality of the drive block influenced test success. Our first round of testing used polylactic acid filament and had the print layers oriented perpendicular to the application of shaker force, increasing the chance of delamination. We updated the print material to a carbon fiber and nylon filament and adjusted the print layer orientation so that the layers were parallel to the shaker force vector. We noticed that the estimated drive voltage required for the supplemental shakers was reduced after installing the new drive blocks, but it is important to note that other small changes, such as slight shaker alignments, could have influenced drive voltage as well.

We began to test the Flight Random vibration flight environment with the shakers imparting force on Part B of the GOBLET. In this configuration, we ran into issues with high required drive voltage. We determined that attaching the shakers to Part A, which is more compliant, might help create the same acceleration at Control Point 2101 with less shaker force (and therefore drive voltage). After we re-attached the drive blocks to the compliant portion of the GOBLET, we completed the test from 75 Hz–800 Hz. Below 75 Hz and above 800 Hz, the smaller supplemental shakers were unable to re-create the environment because of drive voltage limitations.

Lastly, we moved to the Flight Shock environment. Note that in Section 2.0, we provide a time waveform for the shock profile that creates the desired SRS profile. Common practice at LANL is to define the time waveforms for shocks to ensure consistency across different tests. While initializing the multi-axis shock program, we discovered that Simcenter Testlab's Shock & MIMO Shock Control does not allow the user to upload a time waveform for multiple control DoF shocks. Instead, the user must specify the SRS, then the software will generate an arbitrary time waveform. We also found that the software needs all output channels (i.e., the channels sending drive voltage to shakers) to be located on the same card in the data acquisition unit for shock testing, likely due to time synchronization. With only three shakers in this test, we were able to use a three-output card in our SCADAS data acquisition system, but this limit will be a problem for tests with more than three shakers. In our MIMO setup, the shock pulses had difficulty with accurate control and resulted in an over-test.

Results

Figure 8 shows the control performance for each DoF at the 270 Leg in comparison to the specification for the Transport Random environment. In single-axis testing, each of these tests was performed sequentially, resulting in independent data acquisition for each axis. For quantitative comparison of the specification and control performance, Table 2 reports the

G_{RMS} values for the specification, previously shown in Table 1, compared to the G_{RMS} values of the signal measured at the control location. Note that the G_{RMS} values of the MIMO specifications are lower than the SISO specifications because of truncation to a 20-Hz minimum control frequency. A positive percent difference between the specification and control G_{RMS} indicates an over-testing of the system in the respective axis, while a negative percent difference indicates an under-test. Similar analysis of the control performance and G_{RMS} values for the Flight Random environment are presented in Figure 9 and Table 3, respectively. Truncation to 20 Hz–1000 Hz of the Z-axis results in a decreased G_{RMS} value for the

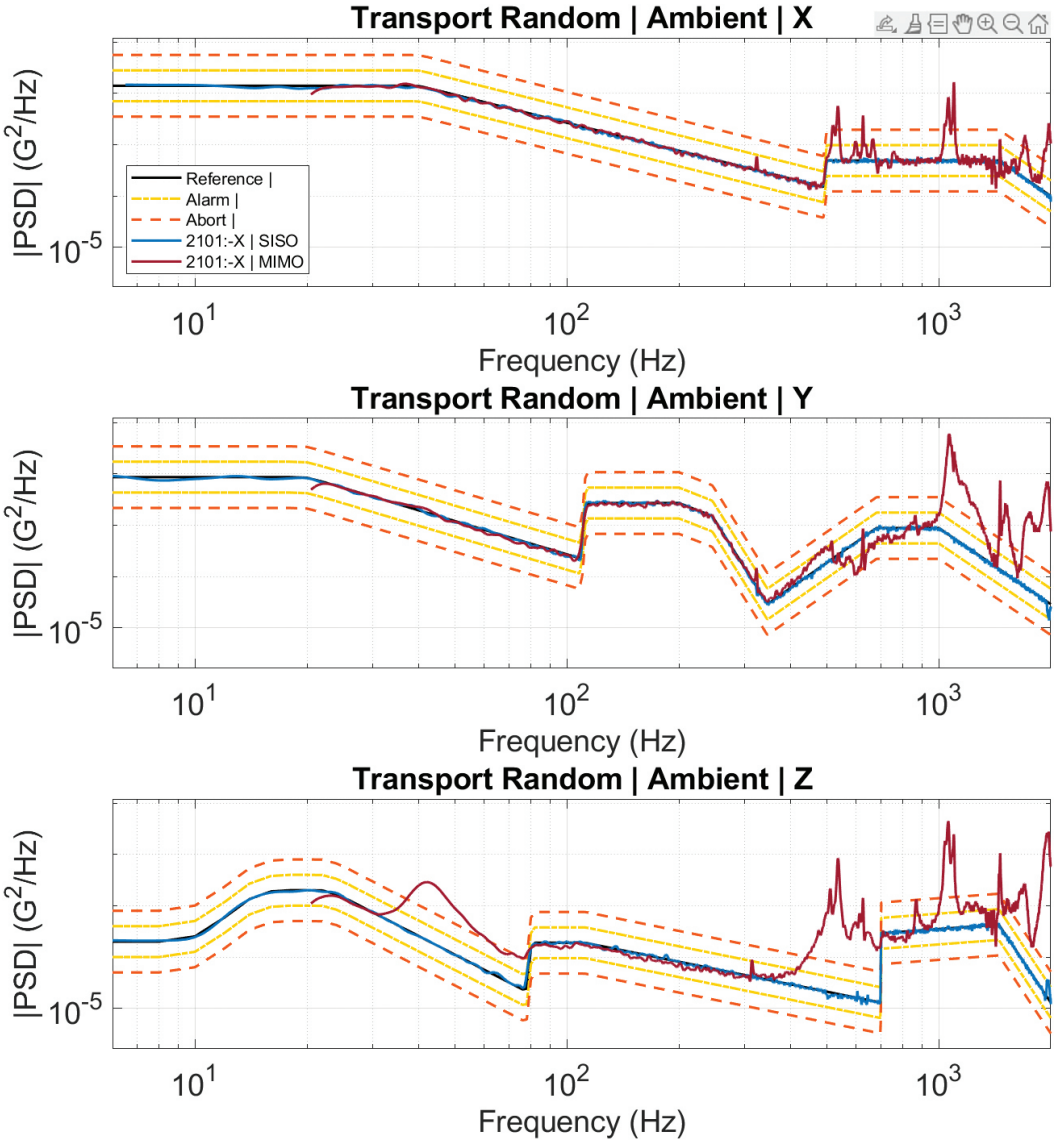

Fig. 8 Control PSD performance comparison for the Transport Random environment

Table 2 GRMS Comparison at Control Point 2101 for the Transport Random environment

	Channel Direction	Specification(GRMS)	Control(GRMS)	% Difference
Single-Axis	X	1.29	1.27	-2.00
	Y	1.11	1.09	-1.27
	Z	0.64	0.63	-0.79
Multi-Axis	X	1.22	1.44	16.5
	Y	1.04	2.20	71.6
	Z	0.62	2.05	107

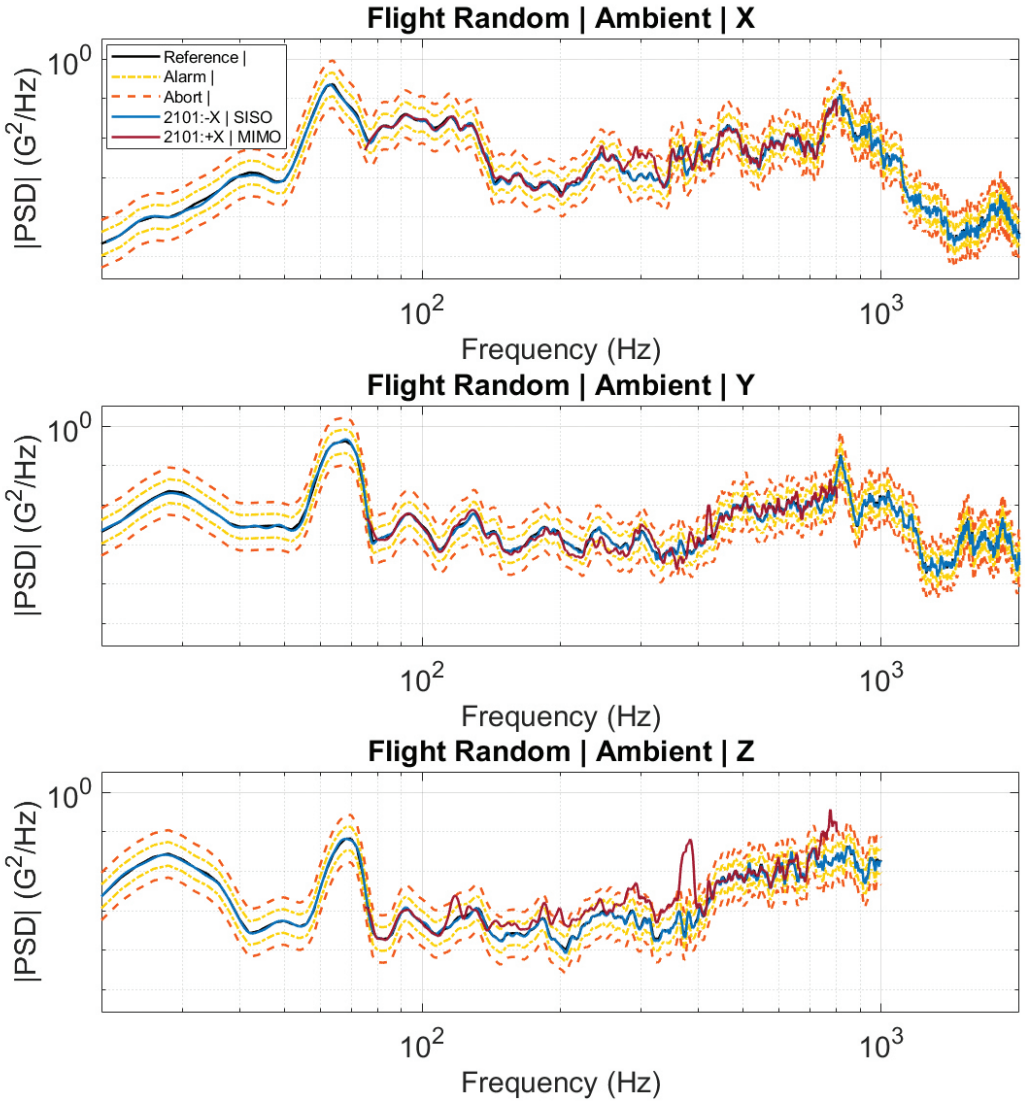

Fig. 9 Control PSD performance comparison for the Flight Random environment

Table 3 GRMS Comparison at Control Point 2101 for the Flight Random environment

	Channel Direction	Specification(GRMS)	Control(GRMS)	% Difference
Single-Axis	X	3.89	3.82	-1.77
	Y	4.16	4.10	-1.59
	Z	3.08	3.04	-1.36
Multi-Axis	X	2.63	2.70	2.63
	Y	2.09	2.25	7.37
	Z	2.19	3.79	53.5

SISO specification compared to Table 1, and truncation of the MIMO specification to 75 Hz–800 Hz further decreased specification G_{RMS} values.

Figure 10 compares the SRS between specification and test for the post-boost shock environment. Visual deviation of the test SRS profile from the reference SRS indicates over-testing or under-testing of the system. As discussed in Section 4.0, we controlled to the time waveforms for the shock environment, so Figure 11 shows the reference and test time data. While the SISO configuration controlled close to the specification value, seen in Figure 3, the MIMO configuration contains a significant spike in maximum acceleration of up to 16.1 G in the Y-axis, far higher than the maximum Y-axis specification

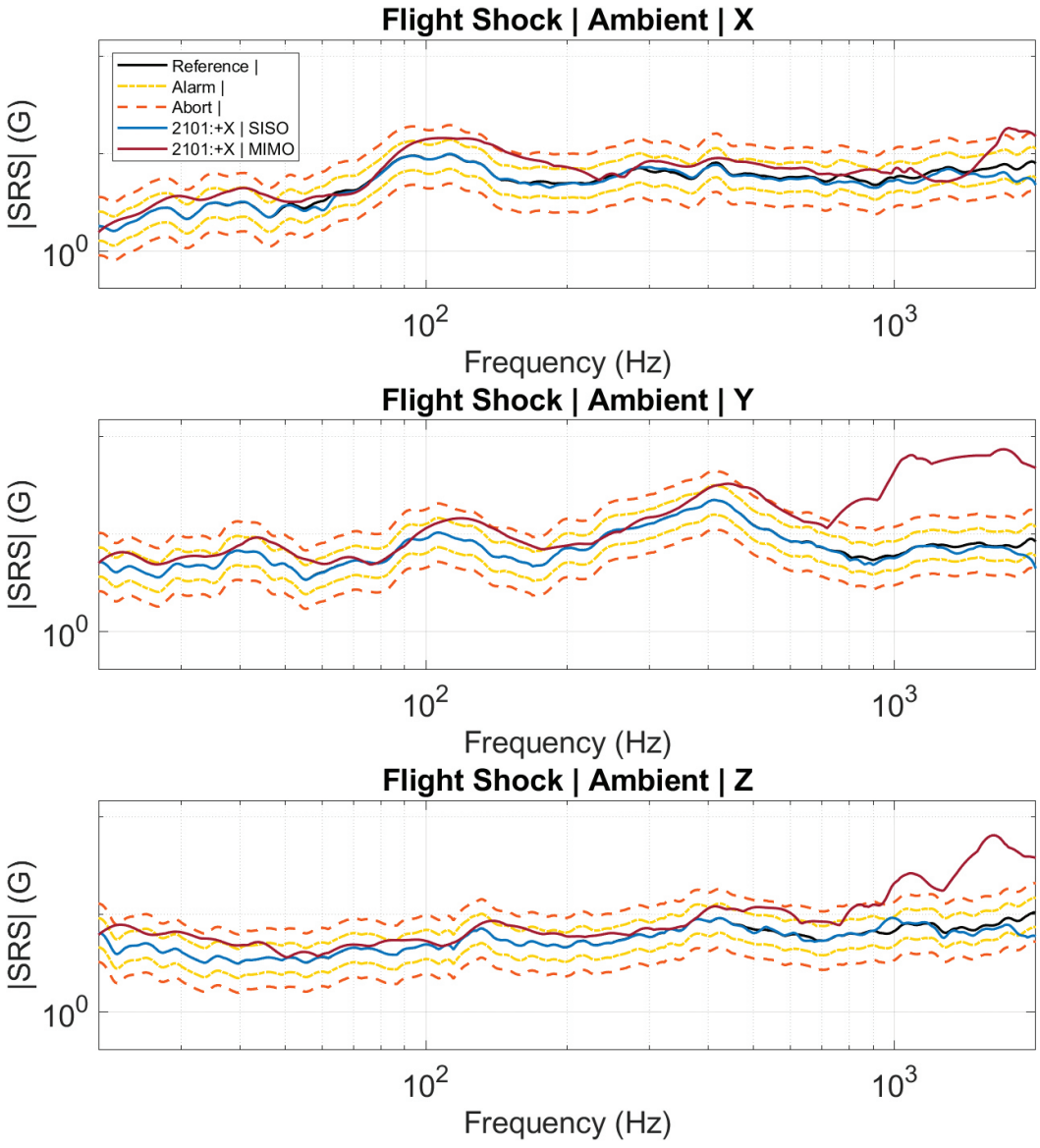

Fig. 10 SRS performance comparison for the Flight Shock environment

acceleration of 3.08 G. Comparison between these waveforms is difficult because the Simcenter Testlab software adds a buffer to the waveform, shifting the pulse further back in time.

In addition to assessing control performance, we evaluated the response at a non-control point of interest, Point 2504 (Figure 4). Instead of analyzing PSDs, we chose to evaluate the transmissibility between the control DoFs at Point 2101 and the in-axis response DoFs at Point 2504. Transmissibility computes the relative acceleration between a control and response channel and contains both amplitude and phase. Peaks in transmissibility amplitude correspond to system resonances, where there is higher acceleration at a response channel than at the control channel. Transmissibility phase describes the relative timing of the acceleration between control and response channels as a function of frequency. For example, a phase of 0° means the two channels are in phase, or exhibiting rigid-body motion. A phase not equal to 0° means the two channels are out of phase, or exhibiting flexion.

Coherence, plotted from 0 to 1 as a function of frequency, examines how much of the response channel data is explained by the measured control signal(s). For MIMO testing, we computed multiple coherence, which examines how much of the response channel can be explained by the combined effect of the control signals. This method allows for a distinction between response attributed to control signals and response attributed to noise, though the participation of individual control channels is not identifiable. Drops in coherence have three main causes: (1) dropouts or saturation in reference and/or response signals,

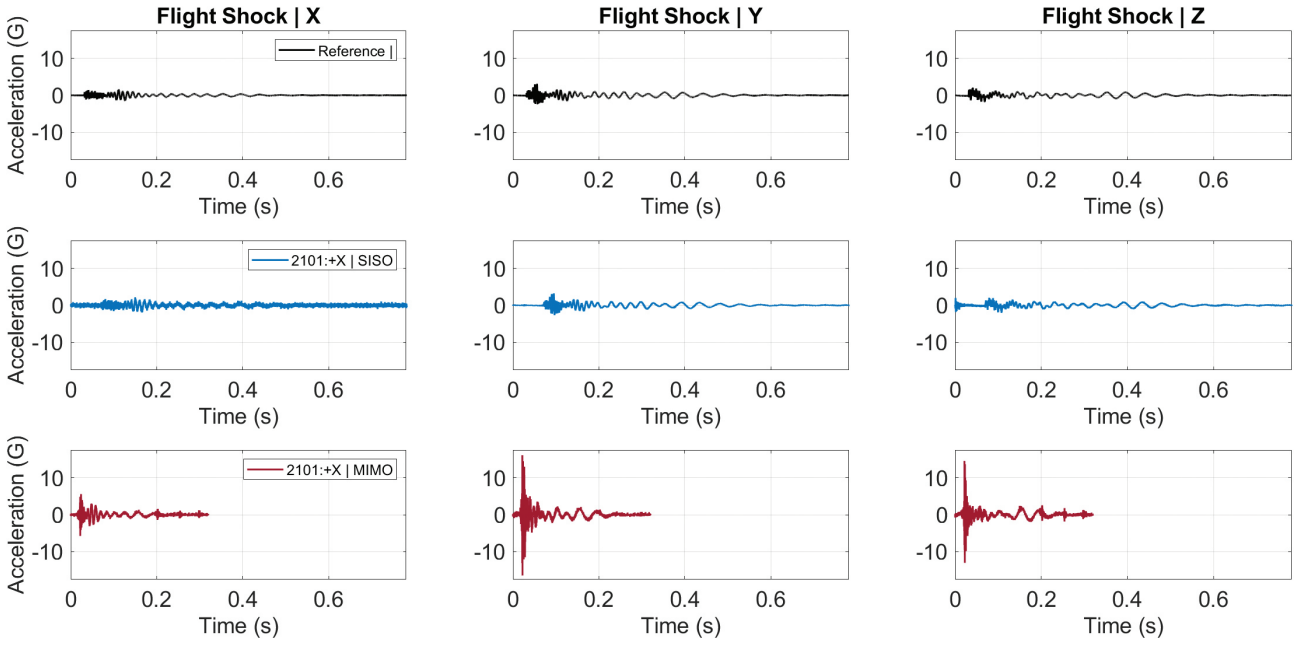

Fig. 11 Time waveform performance comparison at Control Point 2101 for the Flight Shock environment

(2) sensor problems such as faulty hardware or mounting conditions, or (3) system nonlinearity. Most often coherence drops when the response signal is low (e.g., at a system anti-resonance) or if there is rattling or other nonlinear mechanics in the system. Figures 12 and 13 show the coherence, transmissibility phase, and transmissibility magnitude between the control

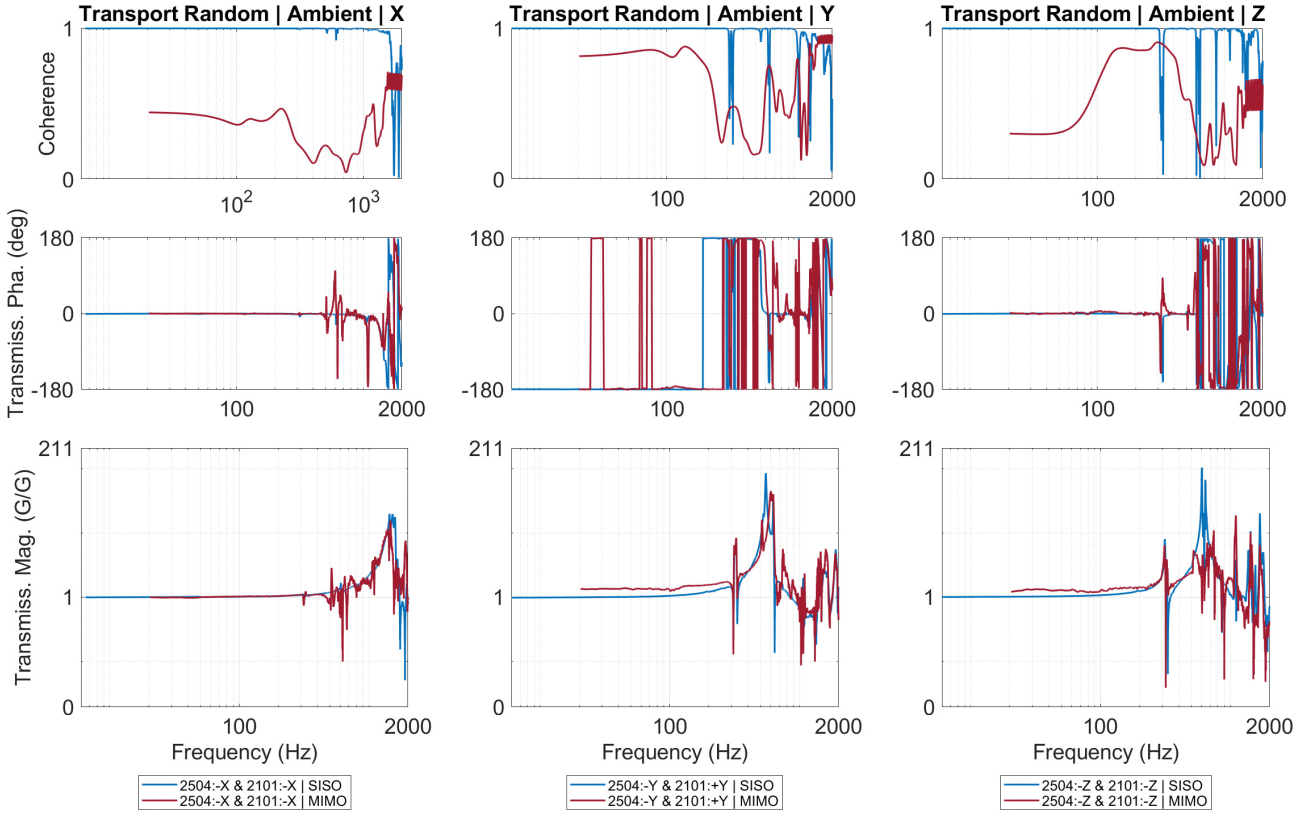

Fig. 12 FRF plots between Points 2101 and 2504 for the Transport Random environment

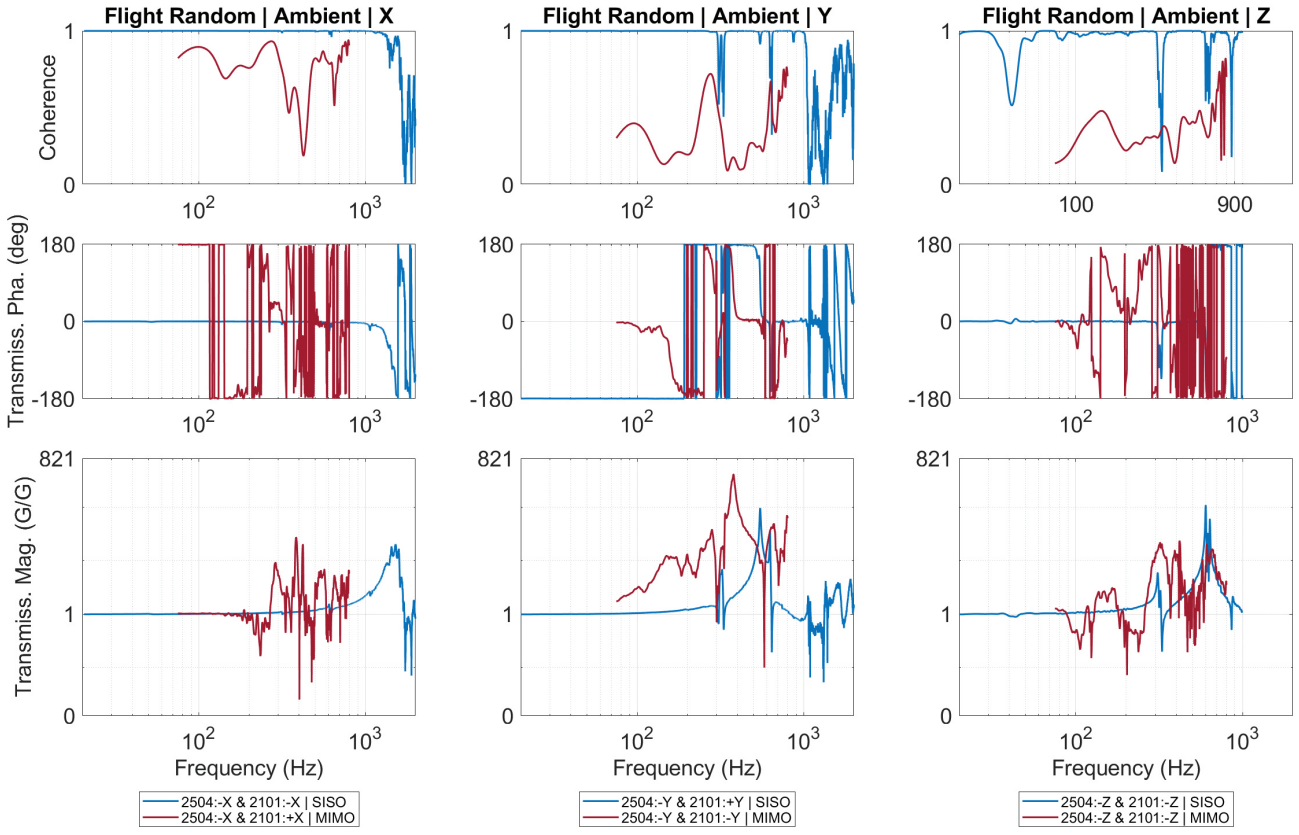

Fig. 13 FRF plots between Points 2101 and 2504 for the Flight Random environment

location (Point 2101) and the location of interest (Point 2504) for the Transport Random and Flight Random environments, respectively.

Discussion

By the G_{RMS} metric used in this study, the SISO tests produced lower control error than MIMO tests for both random vibration environments in all three axes. Interestingly, the SISO configuration resulted in under-tests at all control DoFs for both Transport Random and Flight Random environments, and the MIMO configuration resulted in over-tests. Excitation in other principal axes during each SISO test, also known as cross-axis excitation, may contribute additional energy to the system beyond the specification and lead to an over-test, but this phenomenon was not analyzed during this exploration of the MIMO test method. While it is expected that MIMO tests result in higher control error because of the added complexity of multiple control DoFs, the control performance for the MIMO Transport Random environment was unsatisfactory from 500 Hz–2000 Hz. The control challenges could be a result of many factors such as system resonance, shaker misalignments, shaker attachment locations, or shaker-frame interaction. Because of the limited testing window that we had for this study, we were unable to troubleshoot the poor control accuracy, but we will investigate methods for improvement in future work. Additionally, we plan to investigate strategies for increasing the MIMO frequency range to capture the full qualification environment, as well as analyzing cross-axis response from the SISO testing to better compare the test methods.

The Flight Shock environment had shortcomings in both SISO and MIMO testing. Consulting the shock time waveforms in Figure 11, we notice excessive high frequency content in the SISO X-axis shock pulse, included in the zero-padded signal before the pulse starts and during the ringdown. At first, we suspected an issue with the noise floor of our sensor, but further investigation revealed that the X-axis shock pulse magnitude, although the smallest of all three axes, was not near the noise floor of our control sensor. Next, we investigated whether the Point 2101 X sensor channel was broken. However, investigations revealed that the sensor and data acquisition channel were performing as expected during random vibration testing. Additionally, we replaced the Point 2101 triaxial accelerometer and attempted the shock pulse again; the same issues

remained present. One other source of poor performance could be the Simcenter Testlab shock controller. Unfortunately, the software is proprietary, so we are unable to explore what strategy the controller was using to create this shock pulse. We are interested in exploring the SISO shock control challenges further in future work, because the quality of SISO shocks is important for qualification testing.

As shown in Figure 11, the MIMO shock (maroon line) produced much larger acceleration levels than intended by the shock specification (black line). This over-test would not be acceptable for qualification tests, and future work should investigate whether control for MIMO shock with modal shakers can be improved to levels sufficient for qualification testing. Many factors, such as frame setup, shaker-frame interaction, shaker alignment and/or attachment, shaker location, and control software, could have played a role in the poor control accuracy. Perhaps with commercial MIMO setups, such as the Team Tensor 6 DoF platform, the hardware shortcomings could be less of an issue.

The SRS from both SISO and MIMO shock testing is shown in Figure 10. Comparing the poor performance in the time domain (Figure 11) to the SRS profiles in Figure 10, we note that the SRS alone does not provide enough information about control performance and data quality. For example, the X-axis SISO SRS visually matches the reference profile, with only a slight alarm excursion at 2000 Hz. However, as discussed earlier, the time waveform for the X-axis SISO test exhibited troubling high frequency content and was not considered a success. Likewise, although the MIMO SRS profiles from 700 Hz–2000 Hz exceed the specification, the excursions are visibly less extreme than the accelerations in the time waveform plots in Figure 11. The SRS is the common specification provided by customers for LANL qualification tests, but these findings hint that a different evaluation method should be explored.

The transmissibility magnitude remained similar between SISO and MIMO setups for the Transport Random environment (Figure 12), aside from a missing peak around 500 Hz–600 Hz in the Z axis. Recall that in Section 6.0, we attached the supplemental shakers to the rigid Part B for the Transport Random environment test. Because of this rigidity, it appears that the system dynamics remained similar between SISO and MIMO testing, and the relationship between Points 2101 and 2504 followed the same visual profile. Conversely, the transmissibility magnitude differed greatly between SISO and MIMO setups during the Flight Random environment test (Figure 13). Although we cannot compare dynamics for the full frequency range because of the truncation, within the 75 Hz–800 Hz range, we see many more peaks in transmissibility magnitude (i.e., resonances) for the MIMO test case. These additional resonances could be a result of change in the boundary conditions of the system when the supplemental shakers were mounted to Part A, the comparatively compliant location, for the Flight Random environment. Future work to optimize supplemental shaker attachment locations and better replicate boundary conditions will assist in evaluating the supplemental shaker method.

The transmissibility phase is difficult to evaluate because of sharp jumps between -180° and 180°, but it follows similar trends to transmissibility magnitude. There is less variation between SISO and MIMO for the Transport Random environment test (Figure 12), whereas for the Flight Random environment test (Figure 13), the phase changes occur at lower frequency values for the MIMO test than the SISO test. As we observed with transmissibility magnitude, the addition of shakers to the compliant Part A resulted in more resonances within 75 Hz–800 Hz, so the corresponding phase changes are reasonable.

The coherence between control signals and the response at Point 2504 is significantly lower in the MIMO configuration for both random vibration environments (Figures 12 and 13). Because we computed multiple coherence for the multi-axis tests, this lower value indicates that a large portion of the X-, Y-, and Z-axis response signals cannot be explained by the X-, Y-, and Z-axis control signals. We have not analyzed the coherence of the in-axis control and response signals (known as partial coherence), but it would be an interesting comparison for future work. Furthermore, the supplemental shakers and test frame may have introduced nonlinearities that contributed to the unexplained response signal.

Conclusion

This study aimed to extend previous work in supplemental shaker testing to all three principal axes, performing higher random vibration levels and MIMO shock environments with the assistance of an aluminum test frame. Our previous implementations showed promise for this test method, but area limitations resulted in only achieving two axes of excitation at levels lower than flight environments. In this paper, we present the GOBLET test assembly and relevant shock and vibration environments, describe our supplemental test frame design, conduct SISO tests for three environments to provide a comparison to traditional LANL shock and vibration test methods, and complete an initial three-axis MIMO test series with the supplemental shaker frame.

We learned valuable lessons about test setup during our first supplemental shaker test series. First, if shakers are to be rigidly attached to the test frame there must be other measures taken, such as isolating the shakers with rubber material or using stingers with ball joints to create compliance. Otherwise, the coupling between the frame, shaker, and test article produces too much frame movement and misaligns the shakers. Second, the print material and orientation of the additively

manufactured drive blocks are important for reaching test levels, especially for the Flight Random vibration. Third, the location of supplemental shaker attachment influences the frequency range and acceleration levels that can be achieved, as well as potentially modifying system dynamics. During shock implementation, we encountered some challenges with the Simcenter Testlab control software that may cause issues for future work.

The results presented here represent the first implementation of the new supplemental shaker test frame over a two-week test period. In future work, we aim to increase the tested frequency ranges of random vibration environments, investigate the poor control performance and low coherence during multi-axis tests, use optimization algorithms to inform supplemental shaker attachment locations, explore SISO cross-axis excitation, and develop a consistent MIMO test methodology to move this test method from the research and development (R&D) setting to the qualification setting.

Acknowledgments We would like to thank Lorenzo Placencia for assistance with the GOBLET design, Kirk Webber for strain gauge application on the GOBLET, Thomas Thompson and Kevin Craft for environmental specification development, and Alex Rose for help with supplemental shaker test implementation. This research is funded by the National Nuclear Security Administration (NNSA) Delivery Environments Program.

References

1. P. Daborn, “Smarter Dynamic Testing of Critical Structures,” Ph.D. dissertation, Aerospace Department, University of Bristol (2014).
2. D. Rohe, G. Nelson, and R. Schultz, “Strategies for Shaker Placement for Impedance-Matched Multi-Axis Testing,” in Sensors and Instrumentation, Aircraft/Aerospace, Energy Harvesting & Dynamic Environments Testing, Volume 7, C. Walber, P. Walter, and S. Seidlitz, Eds., pp. 195–212 (2020).
3. S. M. Danforth, S. M. Johnson, K. F. Fenstermacher, A. J. Ramirez, H. R. Sedillo, J. F. Schultze, and E. W. Ferguson, “Developing methods for single-axis base excitation vibration testing with additional distributed shakers,” in ISMA Conference on Noise and Vibration Engineering, pp. 860–871 (2024).
4. C. M. Harris and A. G. Piersol, Harris’ Shock and Vibration Handbook, 5th ed. (McGraw Hill, New York, New York, 2002), pp. 26.19–26.20.
5. H. R. Kramer, J. F. Schulze, S. M. Danforth, and B. P. Mann, “Dynamic Analysis of a Modular Test Stand for Multi-Axis Vibration Testing,” 43rd SEM International Modal Analysis Conference, Orlando, Florida, February 10–13, 2025, Los Alamos National Laboratory document LA-UR-24-30436.